Malaysian Journal of Computing, 9 (1): 1690-1705, 2024

eISSN: 2600-8238

SIR FRACTIONAL ORDER OF COVID-19 BY ADAMS BASHFORTH-MOULTON METHOD

Zubaidah Sadikin[1], Zaileha Md Ali[2*], Fatin Nadira Rusly[3], Nuramira Husna Abu Hassan[4], Siti Rahimah Batcha[5] and Noratika Nordin[6]

[1,2*,3,4,5,6] *College of Computing Informatics and Mathematics, Universiti Teknologi MARA, Selangor, Malaysia.*

[1]zubaidah1590@uitm.edu.my, [2*]zaile597@uitm.edu.my , [3]2020988367@isiswa.uitm.edu.my, [4]2020980613@isiswa.uitm.edu.my, [5]rahimahbatcha@uitm.edu.my, [6]noratikanordin@uitm.edu.my

ABSTRACT

This study addresses a research gap by introducing fractional order derivatives into the SIR model for tracking COVID-19 in Malaysia. The Caputo sense fractional derivative and the Adams Bashforth Moulton method are employed to analyse the COVID-19 behavior and stability. By manipulating fractional order derivative values, this study investigates their impact on key SIR parameters, observing that lower values accelerate the attainment of asymptotic behavior in populations. The stability analysis reveals two equilibrium points: an unstable disease-free equilibrium and a stable endemic equilibrium within the system. This pioneering exploration of fractional order derivatives in the context of Malaysia's COVID-19 modeling contributes valuable insights, enhancing our understanding the behavior of the disease.

Keywords*: SIR, Caputo Fractional Derivative, Covid-19, Adams Bashforth Moulton, Disease stability*

Received for review: 20-11-2023; Accepted: 23-02-2024; Published: 01-04-2024
DOI: 10.24191/mjoc.v9i1.24439

1. Introduction

The Coronavirus disease of 2019 (COVID-19) is a newly found coronavirus that causes an infectious disease (World Health Organization, 2020). COVID-19 was discovered around the end of 2019 in Wuhan, China. According to Albrecht et al. (1996), coronaviruses were initially classified as part of the coronaviridae family because of their crown-like or halo-like appearance. The coronavirus genome comprises a sizeable single-stranded RNA (ribonucleic acid) virus with a lipid envelope studded with club-shaped spike proteins (Britannica, 2021). COVID-19 is the causative agent of SARS (severe acute respiratory syndrome), which scientists discovered to be the source of this infectious disease with cough, fever, exhaustion, and difficulty breathing. When the infected individual coughs or sneezes, the COVID-19 virus is transmitted primarily through droplets of saliva or discharge from the nose.

In late 2019, an outbreak of COVID-19 has spread from one of Wuhan's seafood markets, where some workers have been admitted to a local hospital with pneumonia of unknown cause. The number of patients infected rapidly increases over the next few weeks and spreads beyond the Wuhan region. This uncontrollable situation switched to an epidemic where the number of affected

potentially doubled along with the announcement of WHO based on rising case notification rates. The virus continues to spread widely, and the cases are detected in countless countries worldwide, eventually becoming a pandemic. By 2020, COVID-19 has reached the United States, Europe, and Asia, brought by travellers from affected areas.

Malaysia experienced its initial encounter with COVID-19 on January 25, 2020, when three Chinese tourists were diagnosed with the virus. Despite limited outbreak control measures, the situation escalated rapidly, with confirmed cases jumping from 3 to 22 in just 23 days. A brief respite occurred as no new cases were reported until February 27, 2020. However, this reprieve was short-lived as Malaysia faced a second wave, leading to a surge in daily positive cases, eventually leading the country into a COVID-19 endemic state with a startling three-digit daily case count. As of August 26, 2021, Malaysia had recorded its highest number of cases at 24,599, accompanied by 393 deaths, solidifying its position as one of the hardest-hit countries in Southeast Asia (Idris, 2022). This marked the onset of the COVID-19 pandemic in Malaysia, marked by a significant rise in confirmed cases and the emergence of various clusters.

A study written by Mwalili et al. (2020) focuses on investigating the COVID-19 transmission dynamics, including pathogen in the surroundings and treatment by applying a modified SEIR model. Runge-Kutta methods of fourth and fifth order are used in this study to solve the model equations. The author observed that the R_o in this study is 2.03, indicating that the pandemic will continue in the population without effective control measures such as limiting non-essential travel, social distancing, frequent hand washing, and wearing masks in public.

Mathematical modelling in epidemiology opens a new era in understanding disease transmission and provides recommendations for disease control. A few mathematical models can describe the dynamic of the COVID-19. The Susceptible-Infected-Recovered (SIR) model is a mathematical model used to study the COVID-19 pandemic. In 1927, Kermack and McKendrick developed the model which studied a fixed population with only three compartments, which are susceptible (S), infected (I) and recovered (R). This model started with the number of people in the susceptible, infected, and recovered categories at initial time zero. This SIR model serves as a fundamental mathematical model for transmitting epidemic diseases.

In the article written by Wong et al. (2021), a modified SIR model was used to research a simulation of COVID-19 spread in multiples Malaysian cities under vaccination intervention. Runge-Kutta differential solvers are used in this study to obtain the simulation curve. The author found the curve of active infection varies slightly at different vaccine efficacy levels from this study. The result also shows that lowering the reproduction number is required to maintain the infection curve flat. Hence, a two-pronged strategy, which is compliance with the standard operating procedure (SOP) and vaccination, was suggested in this study to combat the pandemic in Malaysia.

Numerous studies have investigated COVID-19 using various techniques and strategies to comprehend its characteristics and how it spreads. Many researchers have employed methods like Runge-Kutta fourth and fifth order as well as Euler's methods to solve the SIR model, a common tool in epidemiology. Additionally, some researchers have incorporated fractional derivatives, specifically the Caputo derivative, into the model equations. The Caputo derivative is a fractional derivative introduced by Italian mathematician Caputo in 1967. Fractional derivatives represent real or complex derivatives of arbitrary orders in applied mathematics and mathematical analysis, providing a versatile tool for modeling complex phenomena like infectious disease dynamics. Caputo fractional derivative is the most accessible fractional operator to deal with real-world problems because it allows initial and boundary conditions (Atangana, 2018). Applying Adams Bashforth Moulton method to the fractional derivative allows computing the approximate solution. The Adams Bashforth Moulton is obtained from the Adams-Bashforth and Adams Moulton methods. John Couch Adams developed the Adams-Bashforth and Adams-Moulton methods to solve differential equation problems. The Adams-Bashforth method is used as the predictor. In contrast, the Adams-Moulton method is used as the corrector in a multistep process for approximating the solution of a differential equation.

Nabi et al. (2020) used Adam Bashforth Moulton method to solve the fractional SIR model in their research on predicting the evolution of COVID-19 disease in Cameroon. The authors applied Caputo derivative to formulate the fractional model. The result from this study show that the solutions of the fractional model converge to the solutions of the integer model for, and decreasing the fractional-order parameter delays the onset of epidemic peaks, according to numerical simulations. Another study by Tuan et al. (2020) has analyzed the COVID-19 transmission model using Caputo Fractional-order. The authors use Adams Bashforth Moulton method to solve the model equations. The result from this study shows that the pandemic will continue over the next three years based on the R_o and the equilibrium point calculated. However, the authors predicted that more simulations could be presented since the COVID-19 cannot be controlled and the disease's information is always changing. Similar approach has been done by Akindeinde et al. (2022) with Ulam-Hyers criteria to analyze the stability.

In summary, this study uses the SIR model as a mathematical model to solve actual data cases in Malaysia using fractional-order derivatives. The fractional derivatives used are in Caputo sense. The Adams Bashforth Moulton approach is then applied to solve differential equations. This study aims to solve the SIR model using the Adams Bashforth Moulton method, determine the most identical fractional derivative value of SIR model for COVID-19, and analyse the stability of COVID-19 disease in Malaysia.

2. SIR Model Formulation

The SIR models the theoretical number of people infected with an infectious disease over time in a closed population. The name of this group of models comes from the fact that they involve coupled equations connecting the number of susceptible individuals (X), infected people (Y), and recovered people (Z). Individuals move from susceptible compartment to infectious compartment at the rate of β (infectivity rate) and from infectious compartment to recovered compartment at the rate of γ (recovery rate) as shown in Figure 1.

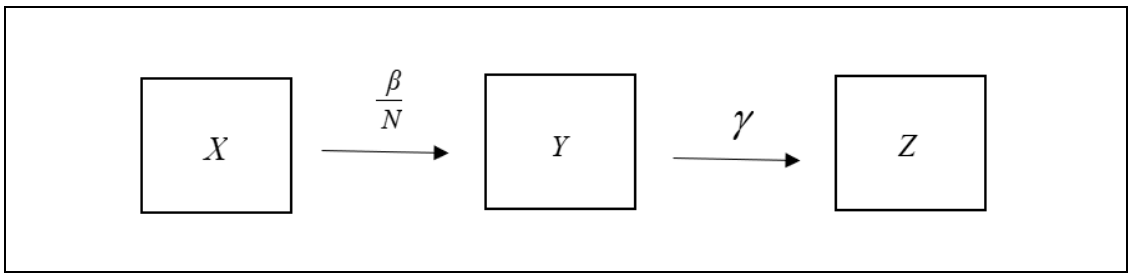

Figure 1. SIR compartment diagram.

Mohd Idris (2022) describes the dynamics of COVID-19 transmission through the following equations:

$$\frac{dX}{dt} = r_0 N - \frac{\beta YX}{N} - \mu_o X + \delta Z \tag{1}$$

$$\frac{dY}{dt} = \frac{\beta YX}{N} - (\mu_o + \mu_1)Y - \gamma Y \tag{2}$$

$$\frac{dZ}{dt} = \gamma Y - \mu_o Z - \delta Z \tag{3}$$

$$N = X + Y + Z \tag{4}$$

where X is the number of susceptible, Y is the number of infectious individuals (symptomatic group), Z the number of fully recovered individuals, N is the total number of people in the area, r_0 the natural birth rate, β is the infectious rate, μ_0 is the natural death rate, μ_1 is the rate of death caused by the disease, δ is the rate at which recovery people become susceptible due to low immunity or health related issues, and γ is the recovery rate.

The SIR model can be dimensionalised by using dimensionless variables, which are

$$X^* = \frac{X}{N},\ Y^* = \frac{Y}{N},\ \text{and}\ Z^* = \frac{Z}{N}$$

Hence, the dimensionless model of the COVID-19 transmission is then given as

$$\frac{dX^*}{dt} = r_0 - \beta Y^* X^* - \mu_0 X^* + \delta Z^* \tag{5}$$

$$\frac{dY^*}{dt} = \beta Y^* X^* - \left(\mu_0 + \mu_1\right) Y^* - \gamma Y^* \tag{6}$$

$$\frac{dZ^*}{dt} = \gamma Y^* - \mu_0 Z^* - \delta Z^* \tag{7}$$

where X^*, Y^*, and Z^* are dimensionless variable for the number of susceptible, the number of infectious individuals and the number of fully recovered individuals, respectively.

2.1 Application of Fractional Caputo Method

Diethelm et al. (2002) discovered a fractional differential equation of the following form in their research:

$$\begin{cases} D_*^\alpha y(t) &= f(t,(y(t)),\ 0 \le t \le T \\ y^{(k)}(0) &= y_0^{(k)}, k = 0,1,...,m-1 \end{cases} \tag{8}$$

where α is the fractional order , $\alpha > 0$, T is a suitable positive number and $m = [\alpha]$ is the first integer not less than α. $D_*^\alpha y(t)$ is the α th-order (always fractional) derivative of y.

Consider y be a function with $(m-1)$ absolutely continuous integer-order derivatives, then the fractional Caputo derivative of order α is defined as:

$$D_*^\alpha\left(y(t)\right) = \frac{1}{\Gamma(m-\alpha)} \int_0^t (t-\tau)^{m-\alpha-1} y^{(m)}(\Gamma)\, d\tau, m-1 < \alpha < m \in Z^+, \tag{9}$$

where $y^{(m)}$ denotes the derivatives of integer m^{th} order of y and in the above integral Γ represents the Gamma function.

Therefore, by using Equation (8) to Equation (5)-(7) the new system of fractional differential equations (FDEs) for the model can be written:

$$D_t^\alpha X^*(t) = r_0 - \beta Y^* X^* - \mu_0 X^* + \delta Z^* \tag{10}$$

$$D_t^\alpha Y^*(t) = \beta Y^* X^* - \left(\mu_0 + \mu_1\right) Y^* - \gamma Y^* \tag{11}$$

$$D_t^\alpha Z^*(t) = \gamma Y^* - \mu_0 Z^* - \delta Z^* \tag{12}$$

2.2 Solution of Fractional Caputo using Adams Bashforth-Moulton

The Equation (8) is equivalent to Volterra integral equation (Brunner, 2017):

$$y(t)=\sum_{k=0}^{m-1} y_0^{(k)} \frac{t^k}{k!}+\frac{1}{\Gamma(\alpha)}\int_0^t (t-u)^{\alpha-1} f(u,y(u))du,\ t\le T \tag{13}$$

For solving the Equation (8) and Equation (13), the fractional Adams method on a uniform grid $\{t_j = jh:\ j=0,1,...,N\}$ with some integer N, step length $h=T/N$, and let $y_j \approx y(t_j)$ was done by Diethelm, et. al (2004). Thus,

$$\begin{aligned} y_{k+1}^p &= \sum_{j=0}^{m-1}\frac{t_{k+1}^j}{j!} y_0^j + \frac{1}{\Gamma(\alpha)}\sum_{j=0}^{k} b_{j,k+1} f(t_j, y_j), \\ y_{k+1} &= \sum_{j=0}^{m-1}\frac{t_{k+1}^j}{j!} y_0^j + \frac{1}{\Gamma(\alpha)}\left(\sum_{j=0}^{k} a_{j,k+1} f(t_j, y_j) + a_{k+1,k+1} f(t_{k+1}, y_{k+1}^p)\right), \end{aligned} \tag{14}$$

where

$$a_{j,k+1}=\frac{h^\alpha}{\alpha(\alpha+1)},\begin{cases} k^{\alpha+1}-(k-\alpha)(k+1)^\alpha, & \text{if} \quad j=0 \\ (k-j+2)^{\alpha+1}+(k-j)^{\alpha+1}-2(k-j+1)^{\alpha+1}, & \text{if} \quad 1\le j\le k \\ 1, & \text{if} \quad j=k+1 \end{cases}$$

and

$$b_{j,k+1}=\frac{h^\alpha}{\alpha}\left((k-j+2)^\alpha-(k-j)^\alpha\right),\ j=0,1,...,k.$$

The initial values are given as

$$D^\alpha X^*(t)=f(t,X(t)), X(0)=X_0,\ 0<\alpha<1, t>0 \tag{15}$$

$$D^\alpha Y^*(t)=f(t,Y(t)), Y(0)=Y_0 \tag{16}$$

$$D^\alpha Z^*(t)=f(t,Z(t)), Z(0)=Z_0 \tag{17}$$

Using Equation (14), the system in the form of Adams-Bashforth-Moulton method is reduced to

$$X_{n+1}^p = X_0^* + \frac{1}{\Gamma(\alpha)}\sum_{j=0}^{n} b_{j,n+1}\left(r_0-\beta Y_j^* X_j^* - \mu_0 X_j^* + \delta Z_j^*\right), \tag{18}$$

$$Y_{n+1}^p = Y_0^* + \frac{1}{\Gamma(\alpha)}\sum_{j=0}^{n} b_{j,n+1}\left(\beta Y_j^* X_j^* - (\mu_0+\mu_1) Y_j^* - \gamma Y_j^*\right), \tag{19}$$

$$Z_{n+1}^p = Z_0^* + \frac{1}{\Gamma(\alpha)}\sum_{j=0}^{n} b_{j,n+1}\left(\gamma Y_j^* - \mu_0 Z_j^* - \delta Z_j^*\right), \tag{20}$$

where

$$b_{j,n+1}=\frac{h^\alpha}{\alpha}\left((n+1-j)^\alpha-(n-j)^\alpha\right),\ 0\le j\le n$$

and

$$X_{n+1} = X_0^* + \frac{h^\alpha}{\Gamma(\alpha+2)}\left(r_0 - \beta Y_{n+1}^p X_{n+1}^p - \mu_0 X_{n+1}^p + \delta Z_{n+1}^p\right) + \frac{h^\alpha}{\Gamma(\alpha+2)}\sum_{j=0}^{n} a_{j,n+1}\left(r_0 - \beta Y_j^* X_j^* - \mu_0 X_j^* + \delta Z_j^*\right), \tag{21}$$

$$Y_{n+1} = Y_0^* + \frac{h^\alpha}{\Gamma(\alpha+2)}\left(\beta Y_{n+1}^p X_{n+1}^p - (\mu_0+\mu_1) Y_{n+1}^p - \gamma Y_{n+1}^p\right) + \frac{h^\alpha}{\Gamma(\alpha+2)}\sum_{j=0}^{n} a_{j,n+1}\left(\beta Y_j^* X_j^* - (\mu_0+\mu_1) Y_j^* - \gamma Y_j^*\right), \tag{22}$$

$$Z_{n+1} = Z_0^* + \frac{h^\alpha}{\Gamma(\alpha+2)}\left(\gamma Z_{n+1}^p - \mu_0 Z_{n+1}^p - \delta Z_{n+1}^p\right) + \frac{h^\alpha}{\Gamma(\alpha+2)}\sum_{j=0}^{n} a_{j,n+1}\left(\gamma Y_j^* - \mu_0 Z_j^* - \gamma Y_j^*\right), \tag{23}$$

where

$$a_{j,n+1} = \begin{cases} n^{\alpha+1} - (n-r_0)(n+1)^\alpha, & \text{if} \quad j=0 \\ (n-j+2)^{\alpha+1} + (n-j)^{\alpha+1} - 2(n-j+1)^{\alpha+1}, & \text{if} \quad 1 \le j \le n \\ 1, & \text{if} \quad j = n+1 \end{cases}$$

3. Stability Analysis

The Jacobian Matrix is used to find the equilibria. Two types of equilibria obtained in this study are disease-free equilibrium and endemic equilibrium. Based on the type of equilibria obtained, we will analyse the stability.

Covid-19 cases in Malaysia from 1 March 2020 to 31 December 2020 are being considered. These data are categorised into three different phases. The duration of phase 1 is 160 days, starting from 1 March 2020 to 7 August 2020. Phase 2 is conducted for 124 days from 1 March 2020 to 2 July 2020. Lastly, phase 3 is 103 days from 20 September 2020 to 31 December 2020 (Mohd Idris, 2022).

Then, the Jacobian matrix is defined from Equation (1) – (3) as

$$J = \begin{bmatrix} -\beta Y^* - \mu_0 & -\beta X^* & \delta \\ \beta Y^* & \beta X^* - (\mu_0+\mu_1) - \gamma & 0 \\ 0 & \gamma & -\mu_0 - \delta \end{bmatrix} \tag{24}$$

3.1 Disease Free Equilibrium

At equilibrium point $E_0 = (1,0,0)$, the Jacobian matrix becomes

$$J = \begin{bmatrix} -\mu_0 & -\beta & \delta \\ 0 & \beta - (\mu_0+\mu_1) - \gamma & 0 \\ 0 & \gamma & -\mu_0 - \delta \end{bmatrix} \tag{25}$$

Hence, the eigenvalues for disease free equilibrium are

$$\lambda_1 = -\mu_0$$

$$\lambda_2 = \beta - \mu_0 - \mu_1 - \gamma$$

$$\lambda_3 = -\mu_0 - \delta$$

3.2 Endemic Equilibrium

At the endemic equilibrium point $E^* = (X_0, Y_0, Z_0)$, the Jacobian matrix is defined as

$$J = \begin{bmatrix} -\beta Y_0 - \mu_0 & -\beta X_0 & \delta \\ -\beta Y_0 & \beta X_0 - (\mu_0 + \mu_1) - \gamma & 0 \\ 0 & \gamma & -\mu_0 - \delta \end{bmatrix} \tag{26}$$

Hence, the eigenvalues for endemic equilibrium are

$$\lambda_1 = -\beta Y_0 - \mu_0$$

$$\lambda_2 = \beta X_0 - (\mu_0 + \mu_1) - \gamma$$

$$\lambda_3 = -\mu_0 - \delta$$

The conclusion made in the stability analysis were based on Woolf et al. (2021). A complete overview of the stability corresponding to each type of eigenvalue is in the Table 1 (Woolf et. al, 2021):

Table 1. Overview of the stability corresponding to each type of eigenvalue.

Type of eigenvalue	**Stability**	**Oscillatory Behaviour**	**Notation**
All real and positive	Unstable	None	Unstable Node
All real and negative	Stable	None	Stable Node
Mixed positive and negative real	Unstable	None	Unstable saddle point
$a+bi$	Unstable	Undamped	Unstable spiral
$-a+bi$	Stable	Damped	Stable spiral
$0+bi$	Unstable	Undamped	Circle
Repeated values	Depends on orthogonality of eigenvectors		

4. Result and Discussion

This section analyses the behaviour of the SIR parameter of COVID-19 actual data using fractional order greater than 0.5. Covid-19 cases in Malaysia from 1 March 2020 to 31 December 2020 are being considered. These data are categorised into three different phases. The duration of phase 1 is 160 days, starting from 1 March 2020 to 7 August 2020. Phase 2 (wave 1) is conducted for 124 days from 1 March 2020 to 2 July 2020. Lastly, phase 3 (wave 2) is 103 days from 20 September 2020 to 31 December 2020 (Mohd Idris, 2022).

4.1 Validation of the Study

The Runge-Kutta build-in method in Matlab software is used to validate the results of simulations solved with the Adams Bashforth Moulton method as in Table 2. The results are in good agreement. Hence, the programming used in this study is valid and reliable.

Table 2. Numerical table of solving SIR model with $\alpha = 1$.

Time (days)	Population					
	Adams Bashforth Moulton			**Runge-Kutta**		
	Susceptible $X^*(t)$	**Infectious** $Y^*(t)$	**Recovered** $Z^*(t)$	**Susceptible** $X^*(t)$	**Infectious** $Y^*(t)$	**Recovered** $Z^*(t)$
0	1.000	0.0010	0.0000	1.000	0.0010	0.0000
5	0.9985	0.0019	0.0006	0.9985	0.0019	0.0006
10	0.9956	0.0036	0.0018	0.9955	0.0037	0.0018
15	0.9900	0.0069	0.0041	0.9899	0.0070	0.0041
20	0.9796	0.0130	0.0084	0.9794	0.0131	0.0085
25	0.9605	0.0240	0.0165	0.9600	0.0243	0.0167
30	0.9265	0.0433	0.0312	0.9256	0.0438	0.0316
35	0.8696	0.0742	0.0571	0.8681	0.0750	0.0578
40	0.7832	0.1178	0.1000	0.7811	0.1188	0.1010
45	0.6694	0.1674	0.1642	0.6670	0.1684	0.1657
50	0.5433	0.2081	0.2495	0.5412	0.2086	0.2512
55	0.4266	0.2258	0.3485	0.4251	0.2260	0.3500
60	0.3333	0.2180	0.4497	0.3323	0.2180	0.4506
65	0.2655	0.1924	0.5430	0.2648	0.1926	0.5435
70	0.2186	0.1595	0.6229	0.2181	0.1599	0.6230

4.2 Analysis of the Results

This study shows the SIR model of phase 1 for 160 days with the values of $\beta = 0.079946685$, $\gamma = 0.046113781$, $\mu_0 = 0$, $\mu_1 = 0.013907432$ and $\delta = 0$ with initial $X^*(0) = 1$, $Y^*(0) = 0.2$ and $Z^*(0) = 0$.

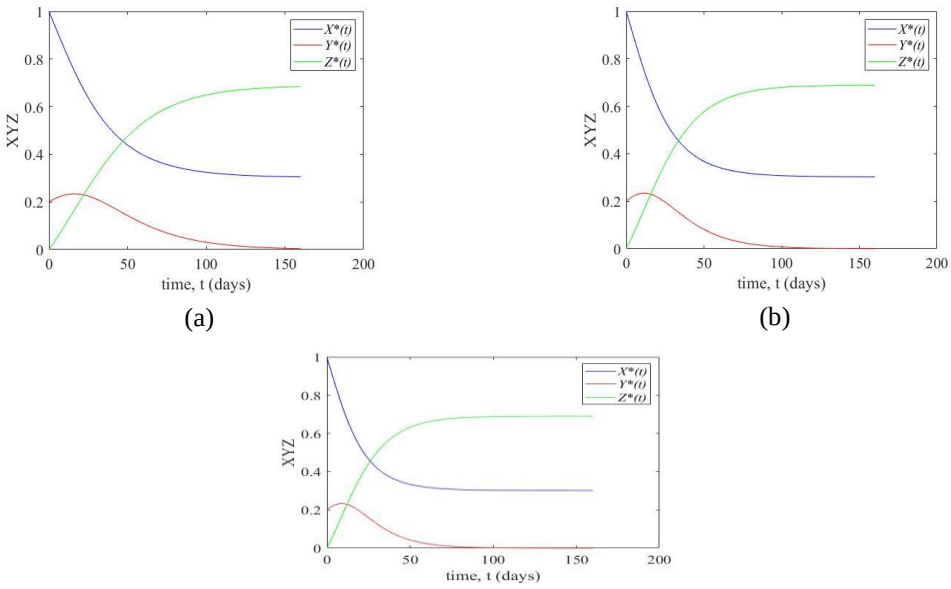

Figure 2. SIR model for Phase 1 COVID-19 with fractional order, (a) $\alpha = 1$,(b) $\alpha = 0.8$ and (c) $\alpha = 0.6$

In Figure 2(a), it is evident that the number of susceptible individuals decreases significantly over a span of 160 days. The infected population, $X(t)$ rises initially but drops after 16 days. Both susceptible, $Y(t)$ and recovered populations, $Z(t)$ exhibit asymptotic behaviour after 156 and 158 days, respectively. Moving on to Figure 2(b), susceptible individuals decrease significantly and reach asymptotic behaviour after 142 days. Conversely, the recovered population increases steadily and approaches asymptotic behaviour after 130 days. Meanwhile, the infected group increases but starts decreasing after 12 days. Figure 2(c) reveals that susceptible individuals fall and reach asymptotic behaviour after 128 days, while the recovered population increases and begins to approach asymptotic behaviour after 120 days. Similarly, the infected population initially rises but then starts to decrease after ten days.

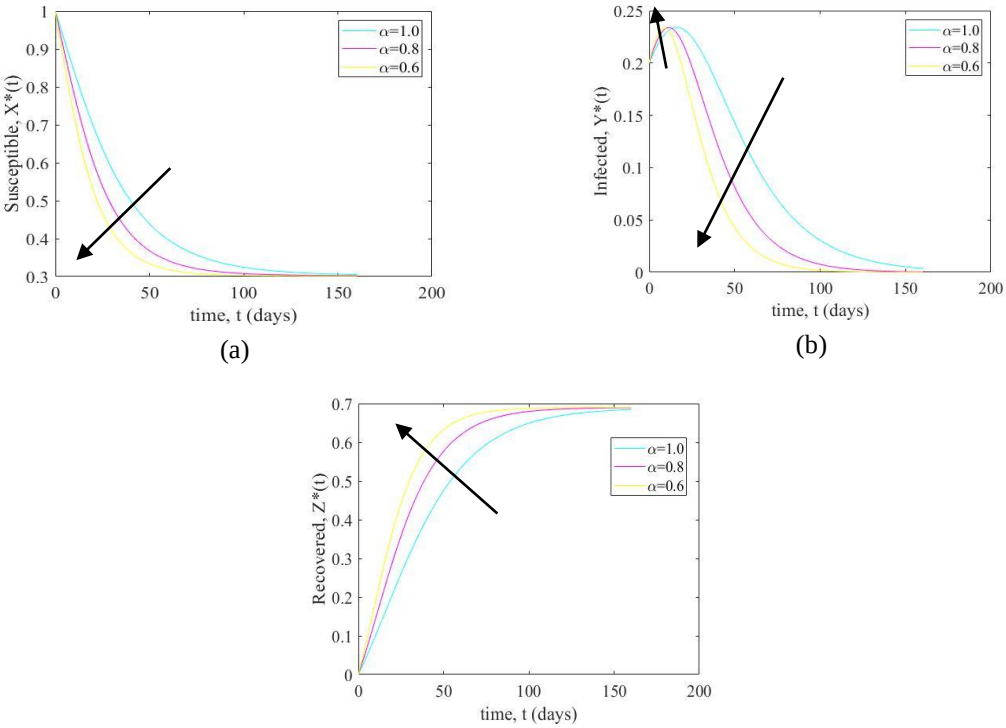

Figure 3. Numerical solution for Phase 1(a) Susceptible, $X^*(t)$, (b) Infected, $Y^*(t)$ and (c) Recovered, $Z^*(t)$ in a time, t (days) with fractional order, $\alpha = 1, 0.8, 0.6$ respectively.

In Figure 3(a), we observe that the time it takes for the susceptible population to reach asymptotic behaviour decreases as the fractional order decreases. Specifically, it takes 156 days for susceptible to reach this state when the fractional order is at its highest, 142 days when it decreases slightly, and 127 days when it decreases further. During this time, the susceptible population decreases and approaches 30 percent of the total population. Moving on to Figure 3(b), we see that as the fractional order decreases, the infected population rises. Consequently, it significantly decreases and approaches zero, especially for lower fractional orders. The peak number of infected cases varies across the three fractional orders, with the peak occurring at 9 days for the highest fractional order, 11 days for the intermediate fractional order, and 16 days for the lowest fractional order. Finally, in Figure 3(c), as the fractional order decreases from its initial value to a lower value, the recovered population increases and approaches 70 percent of the total population. In summary, the figures illustrate how changes in the fractional order impact the dynamics of susceptible, infected, and recovered populations, affecting the time it takes for them to reach asymptotic behaviour and the peak of infected cases.

Phase 2 shows the SIR model for 124 days with the values of $\beta = 0.05158641$, $\gamma = 0.027088421$, $\mu_0 = 0$, $\mu_1 = 0.014122316$ and $\delta = 0$ with initial $X^*(0) = 1, Y^*(0) = 0.2$ and $Z(0) = 0$.

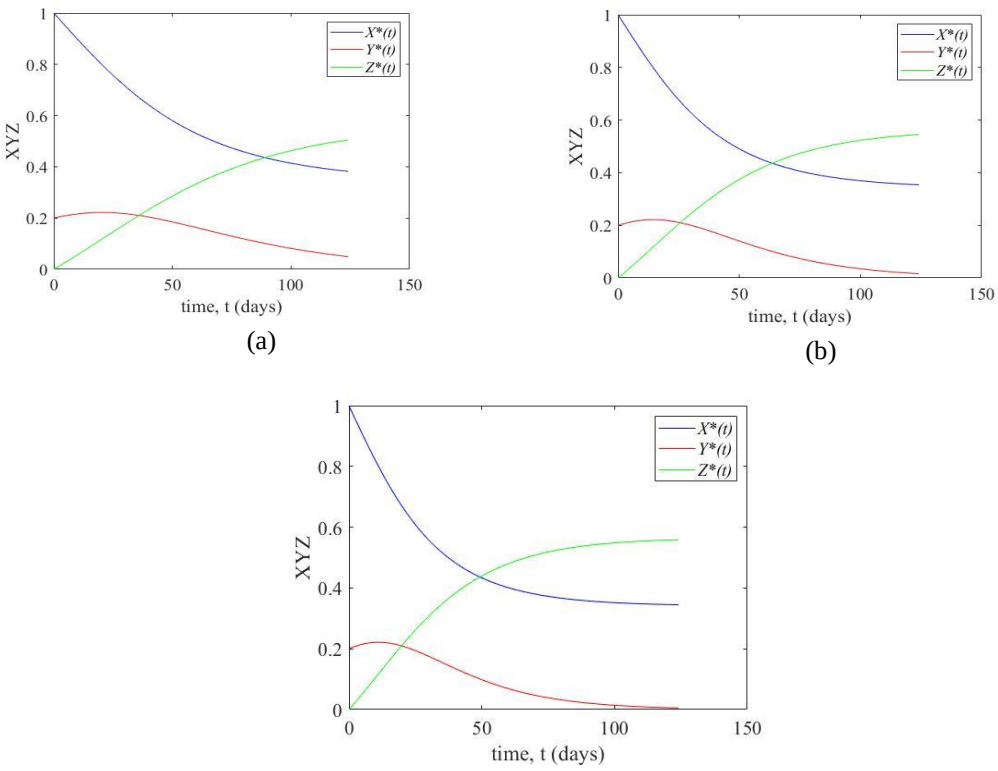

Figure 4. SIR model for Phase 2 COVID-19 with fractional order, (a) $\alpha = 1$, (b) $\alpha = 0.8$ and (c) $\alpha = 0.6$.

In Figure 4(a), we observed a significant increase in the number of infected and recovered individuals, while the susceptible population decreases notably. Additionally, infected individuals start declining after 21 days of disease presence. Meanwhile, Figure 4(b) shows a continuous increase in the number of infected and recovered individuals, with Infected cases reaching an asymptotic level after day 124. On the other hand, the susceptible population experiences a dramatic reduction and only minimally decreases as the interval reaches 110 days. Figure 4(c) illustrates a significant decrease in the susceptible population, while the number of infected and recovered individuals continues to increase. However, after 122 days, infected cases begin to fall and eventually reach an asymptotic state. Comparing these findings to real COVID-19 data in the Figure 4, we can see that the results closely mirror the actual situation. The rapid increase in infected cases, starting on day 15, was primarily due to imported cases and a religious mass gathering involving thousands of people from over 15 countries. Malaysia implemented the Movement Control Order (MCO) on day 18 to curb the spread, leading to a notable improvement in the recovery rate until day 40. Subsequently, as the number of infected cases continued to rise, Malaysia enforced multiple MCOs. However, starting on April 19, 2020, at day 50 of the disease's presence, the number of infected cases began to decrease, eventually reaching single digits on day 115, with only 3 new cases reported on day 124. This trend closely resembles the real data, demonstrating that the simulation's behaviour aligns with the actual situation, particularly with infected cases reaching an asymptotic state after day 124.

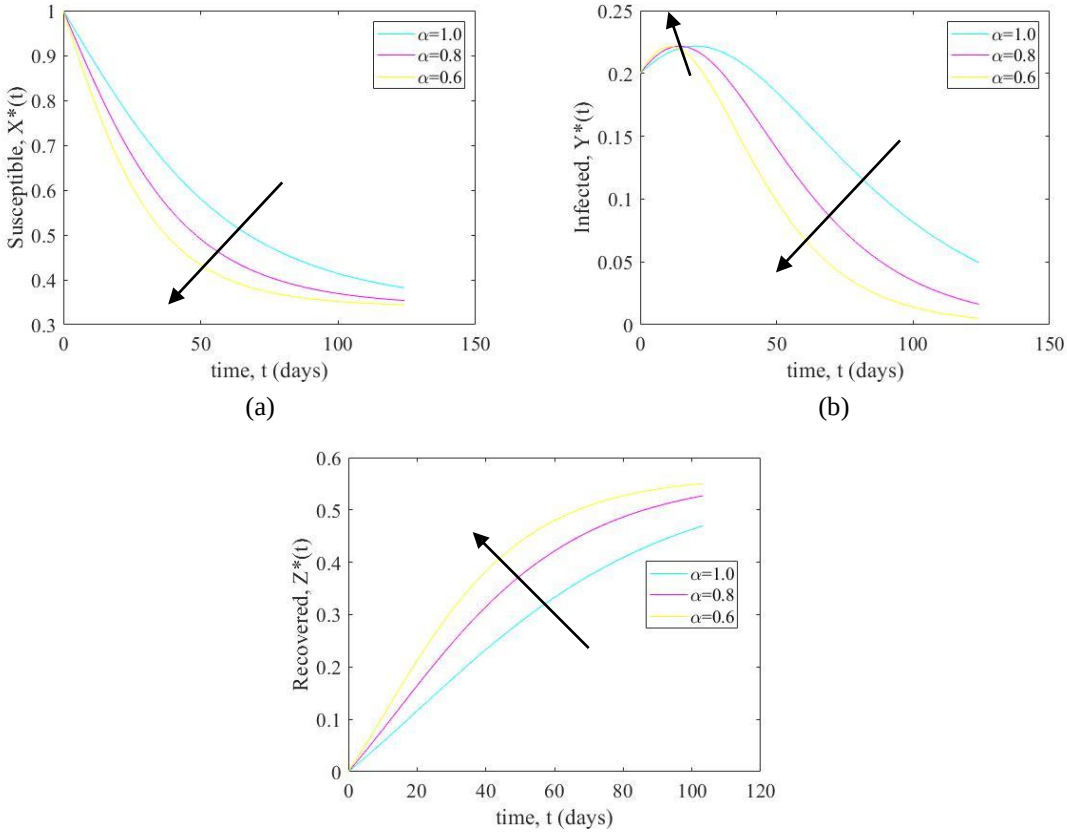

Figure 5. Numerical solution for Phase 2 (a) Susceptible, $X^*(t)$, (b) Infected, $Y^*(t)$ and (c) Recovered, $Z^*(t)$ in a time, t (days) with fractional order $\alpha = 1, 0.8, 0.6$ respectively.

In Figure 5(a), the graph depicting susceptible individuals over time reveals a significant decline within a short time frame. After 120 days of the disease's presence, the number of susceptible individuals stabilizes, exhibiting asymptotic behaviour. For a fractional order value of 0.6, the graph indicates that the susceptible population remains below 40 percent after 100 days of the disease's presence. Moving on to Figure 5(b), it displays a slight initial increase followed by a significant decrease in the number of infected individuals after 30 days, regardless of the fractional order value. Notably, the proportion of infected individuals approaches zero around day 122 of the disease's presence. Finally, Figure 5(c) illustrates a rapid increase in the number of recovered individuals within a short timeframe. The graph also shows that the percentage of recovered individuals is notably higher at day 120. In summary, these figures depict the dynamics of susceptible, infected, and recovered populations over time under different fractional order values. Susceptible individuals decline rapidly and stabilize, infected cases rise briefly before decreasing significantly, and the number of recovered individuals increases rapidly.

Phase 3 demonstrates the SIR model for 103 days with the values of $\beta = 0.262362091$, $\gamma = 0.10316611$, $\mu_0 = 0$, $\mu_1 = 0.003315734$ and $\delta = 0$ with initial $X^*(0) = 1$, $Y^*(0) = 0.9$, and $Z^*(0) = 0.01$.

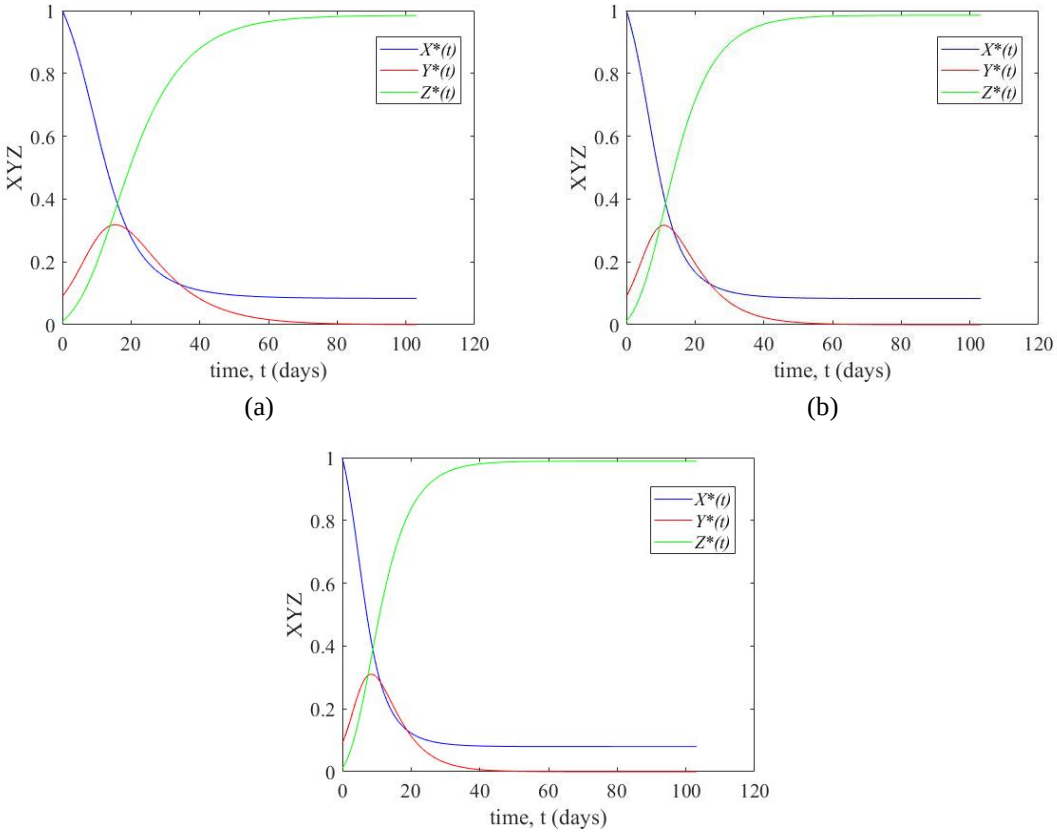

Figure 6. SIR model for Phase 3 COVID-19 with fractional order, (a) $\alpha = 1$, (b) $\alpha = 0.8$ and (c) $\alpha = 0.6$.

In Figure 6(a), we observe a significant decrease in the number of susceptible individuals over time, accompanied by a substantial growth in the recovered population. As for the infected population, it undergoes a dramatic increase after day 20 but then experiences a significant decline after day 20, ultimately reaching an asymptotic state after 85 days. Moving on to Figure 6(b), it shows that the susceptible population decreases rapidly until day 20 and slightly thereafter. Both the recovered and infected populations increase rapidly. However, the susceptible population decreases significantly after ten days of disease absence and reaches an asymptotic state by day 60. In Figure 6(c), the susceptible population undergoes a dramatic decline, particularly in the early period, with a slight decrease after day 20. The graph reveals significant increases in the recovered and infected populations, but then the infected population drops significantly after ten days. These graphs illustrate that the transition to a fractional model is highly sensitive to the order of differentiation. In real-life scenarios, during Phase 3, the number of infected cases increases rapidly, starting from 57 cases on day one and reaching 111 cases on day six. The rapid increase continues, reaching four digits on day 35 due to the Sabah state election on September 26, 2020, leading to new clusters throughout Malaysia. However, infected cases begin to decline after day 61 and reach an asymptotic state by day 63. Recovered cases show consistent growth, with a significant increase on day 42, reaching 1000 cases. Recovery cases continue to increase until day 103. The infected cases exhibit asymptotic behaviour due to a higher recovery rate compared to Phase 2. Therefore, when compared to real infected case data in the Figure 3, the simulation closely resembles the actual situation, particularly in achieving asymptotic behaviour.

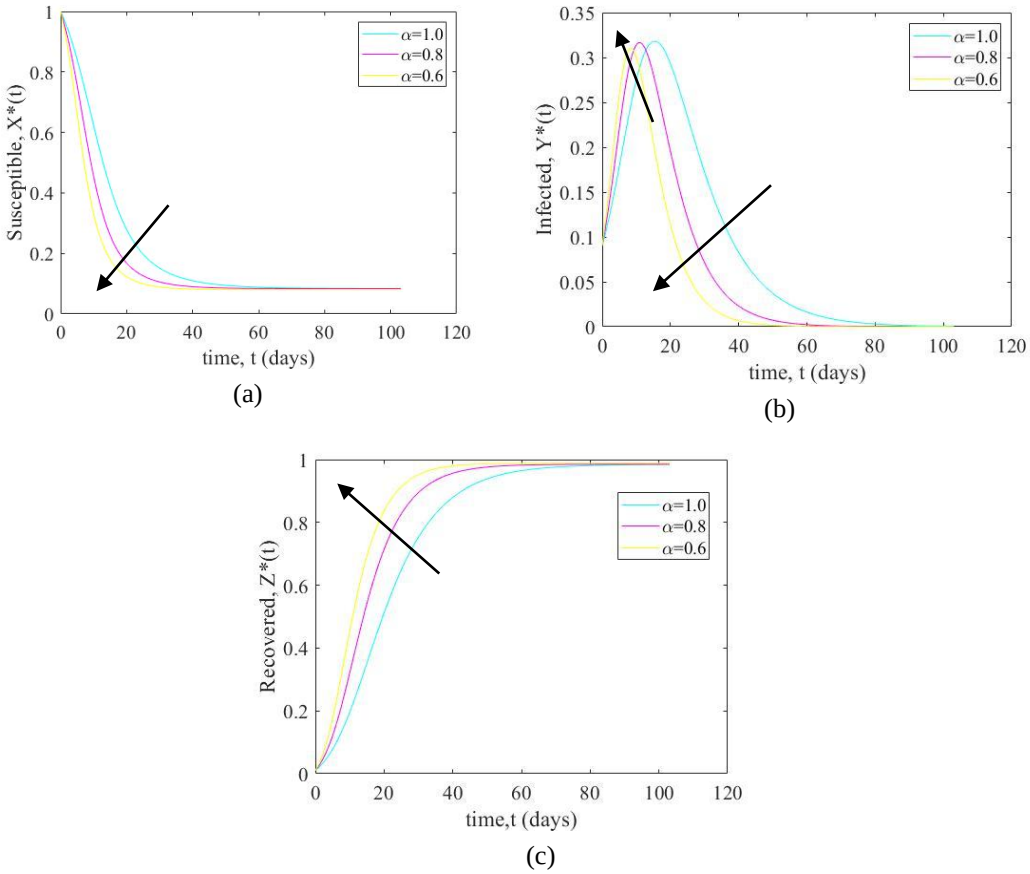

Figure 7. Numerical solution for Phase 3 (a) Susceptible, $X^*(t)$, (b) Infected, $Y^*(t)$ and (c) Recovered, $Z^*(t)$ in a time, t (days) with fractional order $\alpha = 1, 0.8, 0.6$ respectively.

In these figures, we see that as time passes, the number of people susceptible to the disease drops quickly, with about ten percent remaining susceptible after day 50, regardless of the chosen fractional order values. This consistent decrease in susceptibility suggests that the disease's impact lessens over time due to the model's parameters. In Figure 7(b), we witness a significant initial surge in the number of infected individuals, followed by a decline whose extent depends on the chosen fractional order values. This indicates that the choice of fractional order values influences how the infected population evolves, and with a fractional order value of 1, the infected population stabilizes after day 70. Figure 7(c) shows a rapid increase in the number of recovered individuals, slowing down after day 40. Importantly, in all three fractional order scenarios, almost the entire population has recovered by day 70. This implies that the choice of fractional order values may affect the speed of recovery, but significant recovery is eventually achieved for the entire population. In conclusion, these figures provide valuable insights into the dynamics of susceptible, infected, and recovered populations over time, emphasizing the importance of fractional order values. These findings help us better understand infectious diseases and how mathematical models can predict their behavior.

4.3 Stability Analysis

4.3.1 Disease Free Equilibrium

After substituting the data from Mohd Idris (2022), $\beta = 0.079946685$, $\mu_1 = 0.013907432$, $\gamma = 0.046113781$, $\mu_0 = 0$, and $\delta = 0$, the eigenvalues at disease-free equilibrium points are

$\lambda_1 = 0$, $\lambda_2 = 0.019925472$, and $\lambda_3 = 0$. Since the eigenvalues are real numbers with positive signs, the disease-free equilibrium point is unstable.

4.3.2 Endemic Equilibrium

After substituting all the values, the result for phases 1, 2 and 3 are as follow:

Table 3. The Result of Stability for Actual Data.

PHASE 1: Endemic Point (1,0.2,0) $R_0 = 1.733683152$	PHASE 2: Endemic Point (1,0.2,0) $R_0 = 1.904371247$	PHASE 3: Endemic Point (1,0.09,0.01) $R_0 = 2.54310344$
$\lambda_1 = 0$ $\lambda_2 = 0.001968068 - 0.030916438i$ $\lambda_3 = 0.001968068 - 0.030916438i$	$\lambda_1 = 0$ $\lambda_2 = 0.001968068 - 0.020619940i$ $\lambda_3 = 0.001968068 - 0.020619940i$	$\lambda_1 = 0$ $\lambda_2 = 0.0230134$ $\lambda_3 = 0.109254259$
$\alpha = 0$ $\beta = 0.079946685$ $\gamma = 0.046113781$	$\alpha = 0$ $\beta = 0.05158641$ $\gamma = 0.027088421$	$\alpha = 0$ $\beta = 0.26236209$ $\gamma = 0.10316611$
Stability: unstable (unstable spiral)	Stability: unstable (unstable spiral)	Stability: unstable

Table 3 offers a detailed glimpse into the stability analysis of different phases within a mathematical model describing the dynamics of the COVID-19 pandemic. In Phase 1, characterized by an endemic point at (1, 0.2, 0) and a basic reproduction number, R_0 of 1.733683152, the stability assessment reveals eigenvalues with non-zero imaginary parts, indicating a potential for oscillatory behavior. The term "unstable or unstable spiral" underscores the susceptibility of this equilibrium state to perturbations, suggesting a complex, potentially spiralling, trajectory.

Moving to Phase 2, where the endemic point and R_0 remain the same, the eigenvalues exhibit a similar pattern with non-zero imaginary parts. Once again, the system is identified as unstable or an unstable spiral, reinforcing the notion of dynamic and potentially oscillatory dynamics. In Phase 3, marked by a distinct endemic point at (1, 0.09, 0.01) and a higher R_0 of 2.54310344, the stability analysis reveals eigenvalues with a different nature. While one eigenvalue remains zero, the other two have non-zero real parts, indicating a level of instability. In this case, the term "unstable" is used to characterize the equilibrium state.

The interpretation of these results involves understanding the implications of stability or instability in the context of disease spread. Endemic points represent potential equilibrium states within the population, and the associated R_0 values signify the disease's transmission potential. The presence of non-zero imaginary parts in the eigenvalues suggests the possibility of oscillatory behavior, contributing to the overall complexity of the disease dynamics.

In summary, these stability analyses contribute valuable insights into the potential trajectories of COVID-19 spread in different scenarios. The identification of unstable or spiralling behavior underscores the need for careful consideration of dynamic factors when modeling and predicting the evolution of the pandemic. Further exploration of the specific mathematical model and parameter interactions would likely enhance our understanding of the intricacies of COVID-19 dynamics in each phase.

5. Conclusion

In summary, this mathematical study employing the SIR model has achieved its objectives and revealed significant findings. Firstly, the Adams Bashforth Moulton method proved effective in solving the fractional SIR model, a crucial tool for comprehending infectious diseases. Secondly, various fractional order values were investigated to establish the most precise representation of the SIR model for COVID-19 in Malaysia. Fractional order values exceeding 0.5 were chosen for analysis, resulting in key observations for each phase: Phase 1 exhibited a close match to real data, with the susceptible and infected populations reaching asymptotic behaviour after day 133; Phase 2 showed strong alignment with real data, achieving asymptotic behaviour after day 124; Phase 3 closely resembled the real situation, with asymptotic behaviour for susceptible and infected populations attained after day 85. Notably, reducing the fractional order derivative values expedited convergence to asymptotic behaviour for all populations. Thirdly, the study evaluated the stability of COVID-19 in Malaysia, identifying two equilibrium points: the disease-free equilibrium and the endemic equilibrium. The findings suggest that the endemic equilibrium points in all three phases are unstable. Overall, this research underscores the effectiveness of mathematical modelling in comprehending infectious diseases, particularly in the context of COVID-19 in Malaysia. The fractional SIR model, in conjunction with careful selection of fractional order values, has facilitated an accurate representation of disease dynamics, contributing valuable insights into the pandemic's behaviour and stability across different phases.

Acknowledgement

The authors would like to express their gratitude to the College of Computing, Informatics & Mathematics, Universiti Teknologi MARA (UiTM) Shah Alam Selangor Malaysia for the assistance in completing this research.

Funding

The research did not receive any specific funding.

Author Contribution

Author1 and Author2 played a key role in overseeing the article writing and reconfirmed the mathematical analysis, with a focus on SIR model and Fractional Caputo. Author3 and Author4 conducted the research as part of their final year project, contributing to derive the mathematical model and solve using mathematical software, MATLAB. Author5 and Author6 were responsible for crafting the research methodology and conducting fieldwork.

Conflict of Interest

The authors have no conflicts of interest to declare.

References

Akindeinde, S. O., Okyere, E., Adewumi, A. O., Lebelo, R. S., Fabelurin, O. O., & Moore, S. E. (2022). Caputo fractional-order SEIRP model for COVID-19 Pandemic. Alexandria Engineering Journal, 61(1), 829-845. from https://doi.org/10.1016/j.aej.2021.04.097

Albrecht, T., Almond, J. W., Alfa, M. J., Alton, G. G. et al. (1996). *Medical Microbiology* [4th edition]. The University of Texas Medical Branch at Galveston.https://www.ncbi.nlm.nih.gov/books/NBK7782/

Atangana, A. (2018). Chapter 5 - Fractional Operators and Their Applications. *Fractional Operators with Constant and Variable Order with Application to Geo-Hydrology,* 79-112. https://doi.org/10.1016/B978-0-12-809670-3.00005-9

Britannica, T. Editors of Encyclopaedia (2021, December 13). *coronavirus*. Encyclopaedia Britannica. https://www.britannica.com/science/coronavirus-virus-group

Brunner, H. (2017). References. In *Volterra Integral Equations: An Introduction to Theory and Applications* (Cambridge Monographs on Applied and Computational Mathematics, pp. 344-382). Cambridge: Cambridge University Press. https://doi:10.1017/9781316162491.012

Caputo, M. (1967). Linear Models of Dissipation whose Q is almost Frequency Independent—II. *Geophysical Journal International, 13*(5), 529-539. https://doi.org/10.1111/j.1365-246X.1967.tb02303.x

Diethelm, K., Ford, N. J., & Freed, A. D. (2002). A Predictor-Corrector Approach for the Numerical Solution of Fractional Differential Equations. *Nonlinear Dynamics, 29*(2002), 3-22. https://doi.org/10.1023/A:1016592219341

Diethelm, K., Ford, N. J., & Freed, A. D. (2004). Detailed Error Analysis for a Fractional Adams Method. *Numerical Algorithms, 36*(2004), 31-52. https://doi.org/10.1023/B:NUMA.0000027736.85078.be

Mohd Idris, N. A., Mohtar, S. K., Md Ali, Z., & Abdul Hamid, K. (2022). A dynamic SIR model for the spread of novel coronavirus disease 2019 (COVID-19) in Malaysia. Malaysian Journal of Computing (MJoC), 7(2), 1108-1119. https://doi.org/10.24191/mjoc.v7i2

Mwalili, S., Kimathi, M., Ojiambo, V., Gathungu, D., & Mbogo, R. (2020). SEIR model for COVID-19 dynamics incorporating the environment and social distancing. BMC Res Notes 13, 352. https://doi.org/10.1186/s13104-020-05192

Nabi, K. N., Abboubakar, H., & Kumar, P. (2020). Forecasting of COVID-19 pandemic: From integer derivatives to fractional derivatives. *Chaos, Solitons & Fractals, 141*(2020), 110283. https://doi.org/10.1016/j.chaos.2020.110283

Tuan, N., H., Mohammadi, H., & Rezapour, S. (2020). A mathematical model for COVID-19 transmission by using Caputo fractional derivative. *Chaos, Solitons & Fractals, 140*, 110107. https://doi.org/10.1016/j.chaos.2020.110107

Wong, W. K., Juwono, F. H., & Chua, T. H. (2021). SIR Simulation of COVID-19 Pandemic in Malaysia: Will the Vaccination Program be Effective? *Physics and Society; Populations and Evolution*. Retrieved January 9, 2021, from https://arxiv.org/abs/2101.07494

Woolf, P., et al. (2021, December 4). *Using Eigenvalues and Eigenvectors to Find Stability and Solve ODEs*. University of Michigan. Retrieved January 9, 2021, from https://eng.libretexts.org/@go/page/22502

World Health Organization. (2020). *Coronavirus*. Retrieved January 9, 2021 https://www.who.int/health-topics/coronavirus#tab=tab_1